A Potential Off-Target Effect of the Wnt/β-Catenin Inhibitor KYA1797K: PD-L1 Binding and Checkpoint Inhibition

Xavier Thuru, Romain Magnez, Gérard Vergoten, Christian Bailly

Biomedicine Hub

Research Article

Biomed Hub 2023;8:1–9
DOI: 10.1159/000528499

Received: August 31, 2022
Accepted: November 15, 2022
Published online: January 19, 2023

A Potential Off-Target Effect of the Wnt/β-Catenin Inhibitor KYA1797K: PD-L1 Binding and Checkpoint Inhibition

Xavier Thuru[a] Romain Magnez[a] Gérard Vergoten[b] Christian Bailly[a, c]

[a]Inserm, CHU Lille, CNRS, UMR9020 – UMR1277 – Canther – Cancer Heterogeneity, Plasticity and Resistance to Therapies, University Lille, Lille, France; [b]Inserm, INFINITE – U1286, Institut de Chimie Pharmaceutique Albert Lespagnol (ICPAL), Faculté de Pharmacie, University of Lille, Lille, France; [c]Oncowitan, Scientific Consulting Office, Lille (Wasquehal), France

Keywords
Cancer · Drug design · Immune checkpoint · KYA1797K · PD-L1 inhibitor

Abstract
Introduction: The quest for small molecule inhibitors of the PD-1/PD-L1 checkpoint continues in parallel to the extensive development of monoclonal antibodies directed against this immune checkpoint. Drug screening strategies are being set up to identify novel PD-L1 inhibitors. ***Methods:*** A virtual screening based on molecular docking with the PD-L1 protein dimer has been performed to identify a new binder. Binding of the identified ligand to PD-L1 has been validated experimentally using a microscale thermophoresis (MST) assay. The cellular effect of the compound was evidenced using a *fluorescence* resonance energy transfer (FRET) assay based on activation of tyrosine phosphatase SHP-2. ***Results:*** We have identified the potent Wnt/β-catenin inhibitor KYA1797K as a weak PD-L1 binder. Molecular docking suggested that the compound can bind to the interface of a PD-L1 dimer, with a geometry superimposable to that of the reference PD-L1 inhibitor BMS-202. The atypical 2-thioxo-4-thiazolidinone motif of KYA1797K, derived from the natural product rhodanine, plays a major role in the interaction with PD-L1. Binding of KYA1797K to recombinant hPD-L1 was validated experimentally, using MST. The drug was found to bind modestly but effectively to hPD-L1. The FRET assay confirmed the weak capacity of KYA1797K to interfere with the activation of SHP-2 upon its interaction with human PD-1. ***Discussion:*** Collectively, the data show that KYA1797K could function as a weak modulator of the PD-1/PD-L1 checkpoint. This effect may contribute, at least partially, to the reported capacity of the β-catenin inhibitor to downregulate PD-L1 in cancer cells. The work also underlines the interest to further consider the rhodanine moiety as a chemical motif for the design of new PD-L1 binders.

Introduction

Small molecule inhibitors of the PD-1/PD-L1 immune checkpoint are actively searched. Such compounds would complement the armamentarium against cancer, providing orally active immune regulators to treat advanced cancers [1]. At present, the therapeutic arsenal is made exclusively of monoclonal antibodies (mAbs) targeting

Karger@karger.com
www.karger.com/bmh

Correspondence to:
Xavier THURU, xavier.thuru@inserm.fr
Christian BAILLY, christian.bailly@oncowitan.com

PD-1 or PD-L1 [2]. Thirteen mAbs have been registered thus far, targeting PD-1 (ten) or PD-L1 (three), but there is no approved small molecule capable of blocking the checkpoint. Numerous compounds have been identified, principally directed against PD-L1, but none has demonstrated a marked anticancer action in humans. Only a very few PD-1 or PD-L1 small molecule binders have been advanced to clinical trials, such as compounds CA-170 (but it is a dual antagonist of PD-L1 and VISTA) [3, 4] and MAX-10181 (from Maxinovel Pty., Ltd., China) which is a PD-L1 binder currently undergoing phase 1 clinical trial in patients with advanced solid tumor (NCT0412233) [5]. New small molecules targeting PD-L1 are regularly discovered, such as our pyrazolone-type PyrDLones [6] and the pro-drug YPD-30 which was shown recently to bind to PD-L1 and to exhibit significant antitumor activity in vivo [7]. Many other compounds could be cited, all in early preclinical development [8, 9]. These newer molecules remain far from clinical trials at present. Efforts must continue to implement new compounds. Oral medication targeting PD-L1 could be extremely useful to reach tumors not easily accessible to mAbs, such as brain tumors, and to reduce costs of treatment.

Various approaches have been proposed to screen for PD-L1 inhibitors, using experimental and/or computational methods [10]. The knowledge of the tridimensional structure of PD-L1 has greatly helped the identification of compounds capable of binding to the interface of two head-to-head PD-L1 monomers [11–13]. The structural information has been largely exploited to identify new binders, based on biophysical and computational approaches [14, 15], and for the design of PD-L1 binders containing a biphenyl core, such as the compounds initially discovered by Bristol-Myers Squibb like BMS-202 and analogs [16]. There are now different classes of PD-L1 inhibitors, with varied structures and mechanisms of action [17]. For our part, we have exploited two complementary approaches. On the one hand, we set up a biophysical method based on microscale thermophoresis (MST) to characterize drug-PD-L1 interaction and to guide the design of new binders [6, 18, 19]. On the other hand, we set up a molecular docking approach, based on a deconvolution of the biphenyl scaffold originally proposed by BMS, to identify new potential PD-L1 binders [20–22]. The two approaches contributed to the identification of novel PD-L1-binding agents. In the frame of our drug screening effort, we have now identified the compound KYA1797K as a weak PD-L1 binder. This synthetic compound, with an atypical 2-thioxo-4-thiazolidinone motif derived from the natural product rhodanine (Fig. 1), is known as a potent and selective Wnt/β-catenin inhibitor (IC_{50} = 0.75 μM) [23, 24]. We discovered that the compound can also bind to PD-L1, although with a relatively low but non-negligible affinity. The PD-L1-binding characteristics of the compound are reported here and discussed in light of the biological properties of the compound.

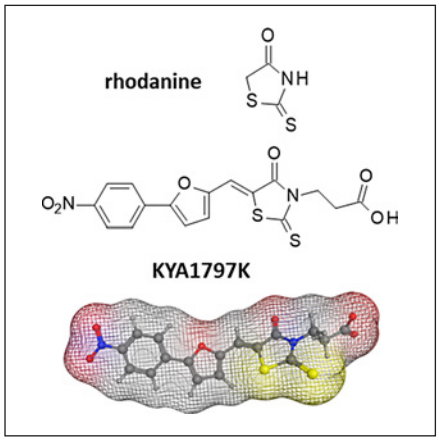

Fig. 1. Structure KYA1797K ($C_{17}H_{11}KN_2O_6S_2$, compound identity number [CID]: 119057297), which derives from the natural product rhodanine, also shown. KYA1797K is a synthetic product, with the following molecular characteristics: Mw = 404.4 Da; total solvent accessible surface area (SASA) = 649.6 Å^2 (hydrophobic SASA = 69.9 Å^2 and hydrophilic SASA = 252.6 Å^2); molecular volume 1,134.7 Å^3; log *p* (octanol/water) = 3.3 and log *S* (aqueous solubility) = −5.2. SASAs were calculated with a probe of 1.4 Å radius. Drug properties were calculated with the BOSS 4.9 software.

Materials and Methods

In silico Molecular Docking Procedure

The procedure used to identify PD-L1-binding small molecules has been reported previously [20, 21]. In brief, the 3D structure of PD-L1 (PDB code 5J89 [25]) was used in docking experiments performed with the GOLD software (Cambridge Crystallographic Data Centre, Cambridge, UK). The structures of the various ligands have been optimized using a classical Monte Carlo conformational searching procedure as described in the BOSS software [26]. The side chain flexibility of amino acids within the hydrophobic pocket (Y56, Y123, M115, D122 for both chains) is taken into account while computing the free energy of hydration (Monte Carlo search) and the empirical potential energy of interaction with the SPASIBA force field. Ligands are defined as flexible during the docking procedure. For each ligand, up to 30 poses that are energetically reasonable were kept while searching for the correct binding mode of the ligand. The decision to keep a trial pose is based on ranked poses, using the PLP fitness scoring function

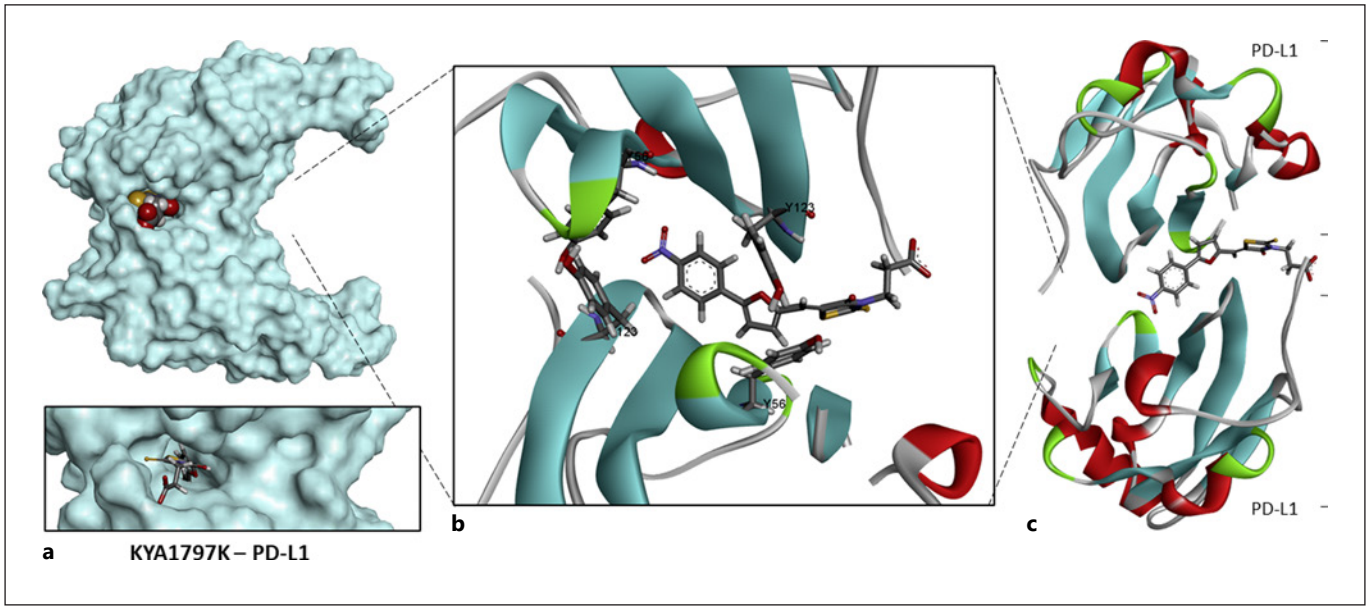

Fig. 2. Molecular model of KYA1797K bound to the PD-L1 dimer. View (**a**) shows the drug located at the interface of the protein dimer. The two protein units (in cyan) sandwiches the drug ligand. The closer view (**b**) shows the compound in the binding pocket, closed by four tyrosine residues (two Y56 and Y123 on each side of the cavity). View (**c**) shows the KYA1797K molecule sandwiched by the two PD-L1 monomers, using a ribbon model with the α-helices (red) and β-sheets (cyan).

(which is the default in GOLD version 5.3 used here). In addition, an empirical potential energy of interaction ΔE for the ranked complexes is evaluated using the simple expression ΔE (interaction) = E (complex) – (E [protein] + E [ligand]). The spectroscopic empirical potential energy function SPASIBA and the corresponding parameters were used [27, 28]. Molecular graphics and analysis were performed using the Discovery Studio 2020 Client software, Dassault Systemes Biovia Corp.

Microscale Thermophoresis

The MST procedure used to quantify inhibition of PD-L1 binding to PD-1 has been described previously [18]. Briefly, MST was conducted using an NT.115 Pico MST instrument (Nano Temper Technologies GmbH) equipped with red and blue filter sets. Recombinant Human PD-L1 His-tag protein (R&D Systems, reference #9049-B7-100), diluted to 200 nM in PBS-T buffer (supplied by the vendor), was labeled with Monolith His-Tag Labeling Kit RED-tris-NTA (Nano Temper). The RED-tris-NTA dye was diluted in PBS-T to 100 nM. The mix was incubated at room temperature in the dark for 30 min. Ligands were diluted with a serial 1:1 ratio of 16 gradients. Then the labeled protein and ligands were mixed with 1:1 ratio and incubated at room temperature in the dark for 15 min. Capillaries are then filled individually and loaded into instrument. Data were acquired using high MST power and 100% LED. Data were analyzed using MO Control Software (Nano Temper). For binding affinity analysis, ligand-dependent changes in MST are plotted as Fnorm values versus ligand concentration in a dose-response curve. Fnorm values are plotted as parts per thousand (‰).

Fluorescence Resonance Energy Transfer

A cellular model was developed using CHO-K1 cells overexpressing the protein of interest, PD-1. The model involves the cellular expression of a PD-1-YFP fluorescent protein (fluorescent emission of acceptor yellow fluorescent protein; λ_{Ex} = 514 nm λ_{Em} = 527 nm) and a second fluorescent protein SHP-2 tagged with CFP (donor cyan fluorescent protein, λ_{Ex} = 433 nm, λ_{Em} = 475 nm). CFP and YFP are variants of the green fluorescent protein (GFP) from *Aequorea victoria* [29]. Src homology 2 (SHP-2) is a tyrosine phosphatase selectively recruited by PD-1 to initiate T cell inactivation [30]. To measure the fluorescence resonance energy transfer (FRET) signal, 10,000 cells co-transfected with the PD-1-SHP-2 vector were used. A Spectramax i3 (Molecular Devices®) was used for the FRET measurements, configured according to the selected fluorochromes with their excitation and emission spectra. Endpoint reading was performed at the center of the well. The reading time is 2 min for a 96-well plate. The drug was tested at various concentrations (typically from 0.5 to 400 μM), and IC_{50} values were calculated by curve fitting using the GraphPad Prism v8 software.

Results

Molecular Modeling of PD-L1/KYA1797K Binding

Two years ago, we initiated in silico analyses of drug-PD-L1 binding with a series of molecules containing a biphenyl unit, as found in the reference products BMS-

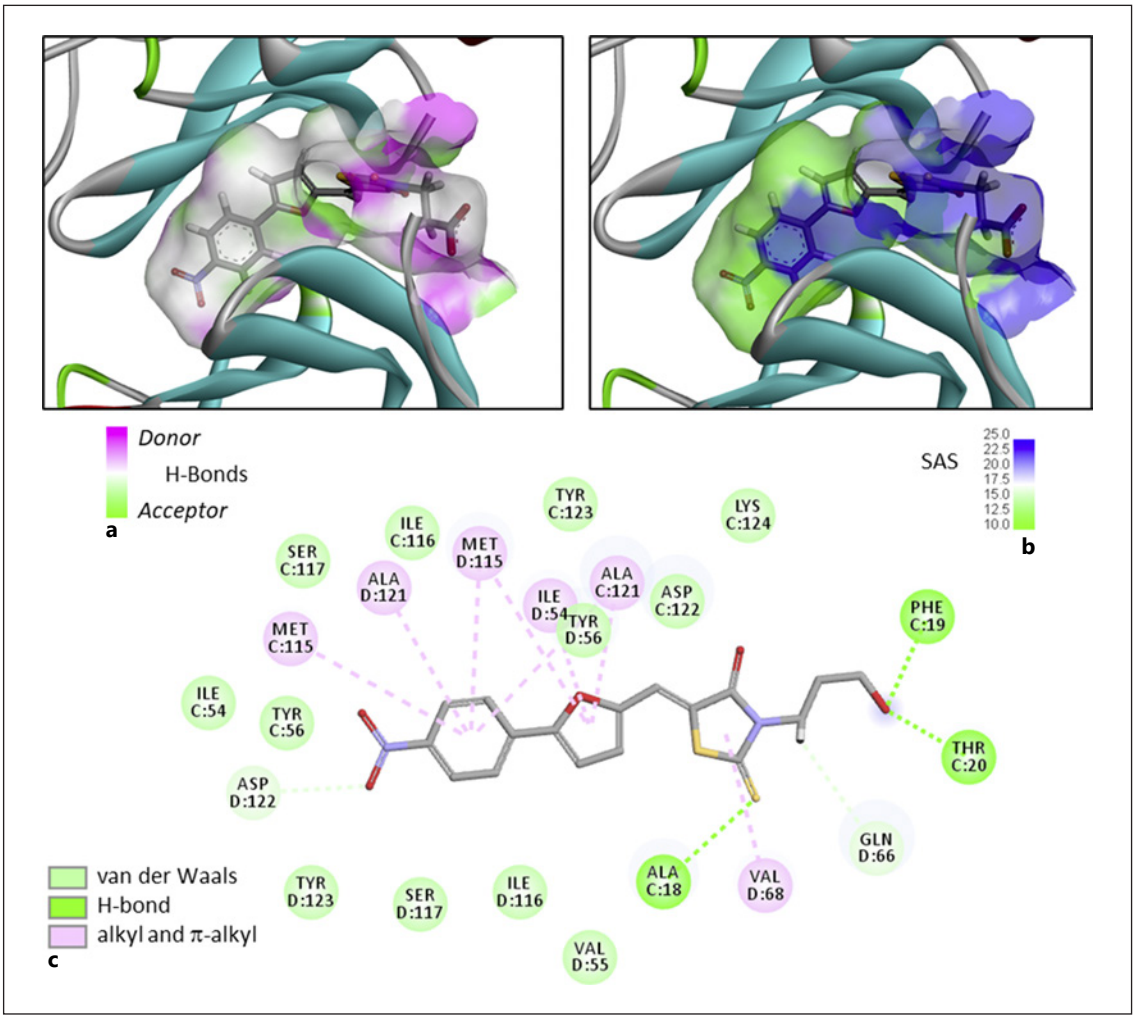

Fig. 3. Detailed views of KYA1797K bound to PD-L1 dimer. The compound inserted into the binding site with (**a**) the hydrogen bond donor (pink) and acceptor (green) sites, and (**b**) the solvent accessible surface (SAS, color code indicated). **c** Binding map contacts for KYA1797K bound to PD-L1 (color code indicated). The calculated potential energy of interaction (ΔE) and free energy of hydration (ΔG) of the KYA1797K/PD-L1 A complex are −91.96 kcal/mol and −29.740 kcal/mol, respectively.

202 and BMS-1166 previously characterized as potent PD-L1 binders [14]. The biphenyl core is an essential element for the binding of the molecules at the interface of the PD-L1 dimeric structure [31]. Different biphenyl-containing molecules binding to PD-L1 were identified, such as the anti-inflammatory drugs flurbiprofen, for example [21]. The unfused bicycle can be extended, without losing affinity for PD-L1. The drug-binding pocket can accommodate longer molecules such as extended p-terphenyl compounds [32] and molecules containing pyridine or imidazopyridine rings, for example [33, 34]. These considerations prompted us to investigate a variety of linear poly-heterocyclic molecules as potential PD-L1 binders.

A molecular docking analysis was performed starting from the crystal structure of PD-L1 bound with the biphenyl molecule BMS-202 which is known to fit well into the binding pocket formed by two adjacent PD-L1 monomers [25]. The PD-L1/BMS-202 complex provides a convenient structural model to look for other potential PD-L1 binders. We selected compounds presenting two essential characteristics: (i) an extended heterocyclic scaffold with at least two or three conjugated aromatics and (ii) a known activity to modulate the PD-1/PD-L1

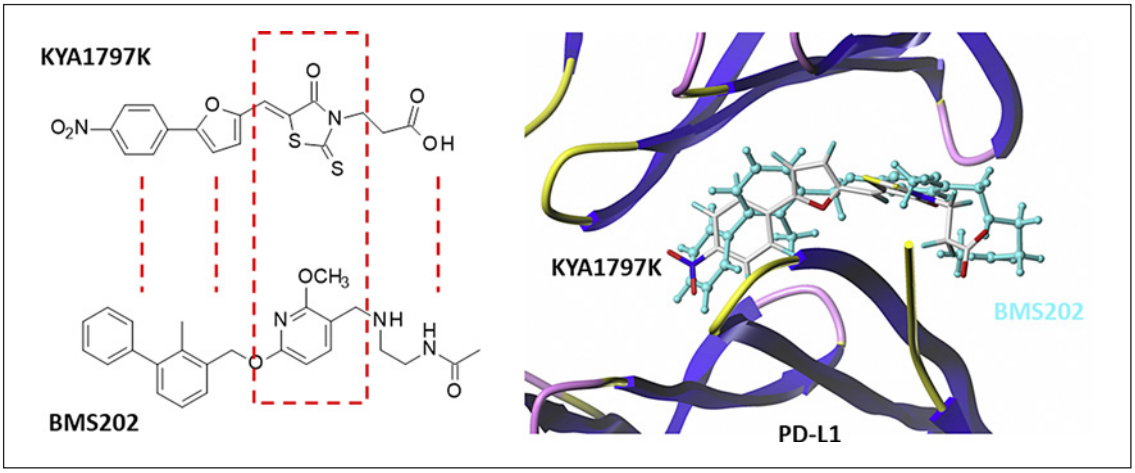

Fig. 4. A superimposed model of KYA1797K and BMS-202 bound to PD-L1 dimer. The rhodanine moiety of KYA1797K occupies exactly the position of the pyridine ring of BMS-202, positioning the phenyl-furan unit in the pocket occupied by the biphenyl moiety of BMS-202. The propionic acid side chain of KYA1797K mimics the terminal acetamido chain of BMS-202.

checkpoint. The capacity of the compounds to bind to PD-L1 was analyzed by molecular docking, using the PDB structure 5J89 as a template [25]. The docking analysis led to the identification of the small molecule KYA1797K as a potential PD-L1 binder. A model of KYA1797K bound to the PD-L1 dimer is presented in Figure 2. The compound fits into the cavity formed by the two juxtaposed PD-L1 monomers, closed on one side by the two tyrosine residues Y123 and Y56. These two residues on each monomer delimitate a pocket in which the phenyl-furan moiety of KYA1797K resides, projecting the thiazolidinone ring toward the surface of the binding pocket, in a zone more accessible to the solvent (Fig. 3). The phenyl-furan moiety of the drug occupies exactly the position of the biphenyl core of BMS-202. The 2-thioxo-4-thiazolidinone motif emerges at the entry of the cavity, positioning the propionate chain toward the external extremity of the binding pocket in an area rich in H-bond donor and acceptor groups (Fig. 4).

The complex between PD-L1 and KYA1797K is stabilized by a panel of molecular contacts, including H-bonds, van der Waals, and π-alkyl interactions (Fig. 3). In particular, the acid moiety and the 2-thioxo group are implicated in H-bonds with the amino acid triad Ala18-Phe19-Thr20. An empirical potential energy of interaction ΔE of −91.96 kcal/mol was calculated for KYA1797K binding to the PD-L1 site, comparable to the energies calculated with BMS compounds (−73.39, −94.80, and −91.31 kcal/mol with BMS-202, BMS-1001, and BMS-1166, respectively). Here the empirical potential energy function reflects the contributions brought by the interaction of atoms which are not covalently bonded, from van der Waals interactions, electrostatic interactions, and hydrogen bonds. The interaction of the 2-thioxo group with Ala18 is important to underline because this residue is known to be essential for the interaction between hPD-L1 and peptides. An A18G mutation was shown to abolish binding of a peptide to PD-L1 [35]. This A18 residue seems to also be a major contributor to the interaction of KYA1797K with PD-L1.

KYA1797K Binding to Recombinant Human PD-L1

The ability of KYA1797K to interact with the PD-L1 protein was evaluated via a specific MST assay using a recombinant human PD-L1 protein commercially available. The results are presented in Figure 5. KYA1797K showed a dose-dependent binding to PD-L1 in solution. A standard monophasic binding curve was observed during the thermophoresis experiments, and a dissociation constant (K_D) of 59 ± 8 μM was calculated. The value is modest compared to that measured with a human anti-PD-L1 antibody (atezolizumab [Tecentriq®], K_D = 92 ± 11 nM) but highly reproducible and significant for such a small molecule. For comparison under strictly identical conditions, the anti-inflammatory compounds nitroflurbiprofen and lonazolac gave K_D values of 114 ± 29 μM and 24.3 ± 2.7 μM, respectively, whereas K_D values in the nanomolar range have been measured with specifically

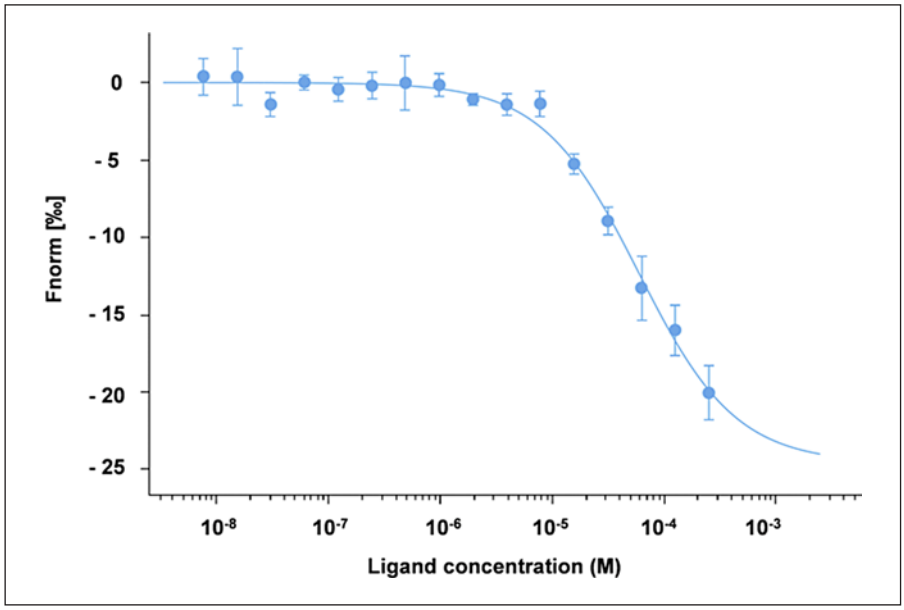

Fig. 5. Dose-response curve for the interaction between His-PD-L1 and KYA1797K. The concentration of His-PD-L1 protein is kept constant at 10 nM, while the ligand concentration varies from 250 μM to 10 nM. Experiments were performed at 22°C with 30 min incubation with high MST and 20% LED power. Signal-to-noise: 25 (noise is defined as standard deviation of difference between responses of experimental data and fitted data. A signal-to-noise ratio of more than 5 is desirable, while more than 12 reflects an excellent assay).

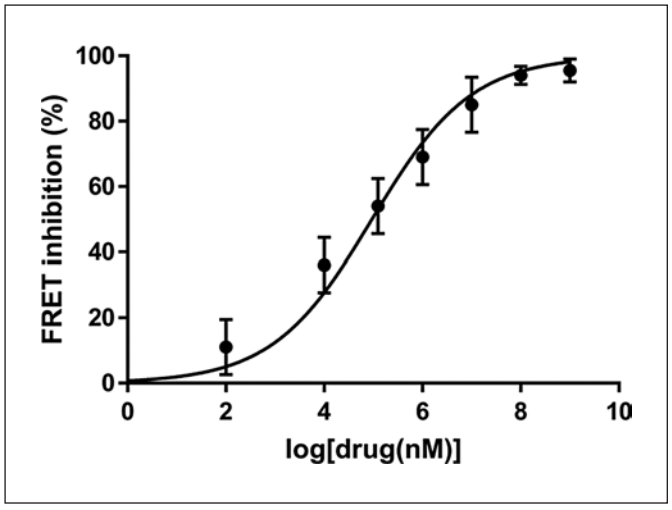

Fig. 6. Dose response of LNZ on FRET signal. The curve shows the effect of increasing LNZ concentrations on PD-1/SHP-2 interaction measured by the FRET assay, from three independent experiments.

designed pyrazole derivatives using the same experimental procedure [6]. This in vitro assay with purified recombinant hPD-L1 confirms that KYA1797K can bind to PD-L1 but with a modest affinity. Next, we investigated the cellular consequence of the interaction.

Inhibition of PD-1 Signaling in Cells by KYA1797K

Binding of PD-L1 to PD-1 triggers a downstream signaling cascade, initiated by the activation of the tyrosine phosphatase SHP-2 upon its interaction with PD-1. We conducted a FRET assay using a pair of fluorescent fusion proteins, SHP-2-CFP and PD-1-YFP (expressed in CHO-K1 cell), for which the emission spectrum of CFP significantly overlaps the excitation spectrum of YFP. During the CFP-to-YFP FRET, there is a quenching of the emission of the donor CFP protein that is directly related to the efficiency of energy transfer and inversely proportional to the sixth power of the distance between the donor and acceptor proteins. It is a powerful method for elucidating protein interactions in many cellular processes and their drug regulation. We used this approach to determine the effect of KYA1797K on PD-1 signaling. The addition of recombinant exogen PD-L1, which binds to cell surface PD-1, triggers a signal (fluorescence transfer) via interaction of PD-1 with SHP-2. The addition of an interaction inhibitor – in our case, a PD-L1 binder – deactivates the signal. A similar method has been developed for high-throughput screening of PD-1/PD-L1 checkpoint inhibitors [36]. As shown in Figure 6, KYA1797K induces a dose-dependent inhibition of the FRET signal. The fitting of the dose-response curve has yielded an IC_{50} of 94 ± 4.2 μM. For comparison, IC_{50} values of 243 μM and 43 ± 4.6 μM were calculated with niflurbiprofen and lonazolac, under identical conditions. Here again, this is weak compared to the effects measured with mAbs, such as a human anti-PD-1 antibody (nivolumab, IC_{50} = 14 ± 4 nM) and a human anti-PD-L1 antibody (atezolizumab, IC_{50} = 47 ± 11 nM). However, the effect observed with KYA1797K is highly reproducible, novel, and important to consider.

Discussion

KYA1797K is a synthetic molecule obtained from the Knoevenagel condensation of a functionalized rhodanine derivative with nitrophenyl-furfural [37]. The compound is a ligand of the regulator of G-protein signaling domain of the axin protein which is essential to control the Wnt/β-catenin signaling pathway. The targeting of the axin-regulator of G-protein signaling domain with KYA1797K leads to a destabilization and degradation of β-catenin and Ras proteins, via activation of protein kinase via GSK3β. As a consequence of this drug-induced degradation process, the compound exerts major anticancer effects against colorectal cancers harboring KRAS mutations [24, 38]. This mechanism is useful to reduce or to avoid drug resistance (notably resistance to anti-EGFR therapeutics like cetuximab and gefitinib) in KRAS-mutated colorectal cancer and in non-small cell lung cancer [39, 40]. The process has been evidenced in leukemia also [41, 42], and the same mechanism can operate in gastric cancer, triple-negative breast cancer, and pancreatic cancer, reducing resistance to standard chemotherapy (FOLFOX, gemcitabine) [43–45]. The compound has been used as a pharmacological tool to block the Wnt/β-catenin pathway in different studies [46–49]. KYA1797K represents a prototypic inhibitor used to modulate the Wnt/β-catenin signaling pathway in various cancer models [50, 51].

In these different pharmacological studies, the compound is classically used in the 5–50 μM range for in vitro studies. It is qualified as a potent and selective Wnt/β-catenin inhibitor (IC_{50} = 0.75 μM), but the maximal effects are usually reported using the compound at 25 μM in many cases [23, 52]. For in vivo studies with xenograft cancer models, KYA1797K was injected intraperitoneally at a dose of 25 mg/mL/day daily [43], but the pharmacokinetic properties of the compound have not been reported. Apparently, the drug is safe and no off-target effect has been reported. It is considered a highly selective Ras destabilizer. A possible contribution of PD-L1 binding to the mechanism of action of KYA1797K is not known at present. However, it is remarkable to note that KYA1797K has recently been shown to downregulate PD-L1 in colon cancer stem cells. The compound was found to inhibit glycosylation and stability of PD-L1, via inactivation of the β-catenin/STT3 signaling pathway [52]. STT3 is the subunit of oligosaccharyl transferase (OST) which harbors the catalytic center of the enzyme. The authors demonstrated that inhibition of β-catenin/STT3 by KYA1797K reduced the stability of PD-L1, thereby inhibiting immune evasion and inducing apoptosis of colon cancer stem cells [52]. No direct PD-L1 effect was mentioned, but we can now postulate that there may be a combination of indirect (axin mediated) and direct (PD-L1 dependent) effects, at least in the in vivo experiments when the drug was injected *ip* at a high daily dose for an extended period (KYA1797K was given at 15 μg/mouse, 6 days/week for 7 weeks). It will be interesting to investigate this option.

The approach deployed here to discover a novel PD-L1 binder can be underlined. On the one hand, the combination of a docking analysis followed with an experimental validation has proved useful to identify KYA1797K as a new PD-L1 binder. This approach can thus be recommended. On the other hand, we must admit that the docking study has largely overestimated the binding PD-L1 capacity of KYA1797K. The calculated empirical potential energy of interaction appeared unreliable, with a ΔE value largely overestimated compared to the affinity measured experimentally. The docking process helped identify the binding site, but it provided only an approximation of the free energy of binding. This is not entirely surprising as conventional structure-based molecular docking methods largely depend on the accuracy of scoring or energy functions for each pose of the protein-ligand docking complex. Other methods and models can be used to improve accuracy of the docking, such as convolutional neural network-based model, for example [53].

Beyond the compound KYA1797K itself, the study also raises novel ideas for the design of PD-L1 inhibitors. The atypical 2-thioxo-4-thiazolidinone motif of KYA1797K is not frequently used in drug design strategies and rarely found in commercially available drugs. This motif certainly warrants further investigation and could represent a novel starting point to build immune suppressors targeted against PD-L1. Recently, antiviral compounds with a similar furanyl-methylidene-rhodanine core have been described [54]. It would be interesting to investigate their capacity to bind to PD-L1 and to modulate the activity of the PD-1/PD-L1 checkpoint.

In conclusion, we have identified the β-catenin inhibitor KYA1797K as a weak PD-L1 binder capable of modulating the functioning of the PD-1/PD-L1 checkpoint. The potency of the compound is modest, but the effect is noticeable and should be kept in mind when using the compound in biological systems. The study also points to the interest of the rhodanine motif as a building element for drug design.

Statement of Ethics

Ethics approval was not required for this in vitro study (no animal study, no human samples used, and no clinical investigation).

Conflict of Interest Statement

The authors have no relevant financial or nonfinancial interests to disclose.

Funding Sources

The authors declare that no funds, grants, or other support were received during the preparation of this manuscript.

Author Contributions

All authors contributed to the study conception and design. Material preparation and data collection and analysis were performed by Xavier Thuru, Romain Magnez, and Gérard Vergoten. The first draft of the manuscript was written by Christian Bailly, and all authors commented on previous versions of the manuscript. All authors read and approved the final manuscript.

Data Availability Statement

All data generated or analyzed during this study are included in this article. Further inquiries can be directed to the corresponding author.

References

1 Yamaguchi H, Hsu JM, Yang WH, Hung MC. Mechanisms regulating PD-L1 expression in cancers and associated opportunities for novel small-molecule therapeutics. Nat Rev Clin Oncol. 2022;19(5):287–305.
2 Yi M, Zheng X, Niu M, Zhu S, Ge H, Wu K. Combination strategies with PD-1/PD-L1 blockade: current advances and future directions. Mol Cancer. 2022;21(1):28.
3 Sasikumar PG, Sudarshan NS, Adurthi S, Ramachandra RK, Samiulla DS, Lakshminarasimhan A, et al. PD-1 derived CA-170 is an oral immune checkpoint inhibitor that exhibits preclinical anti-tumor efficacy. Commun Biol. 2021;4(1):699.
4 Sasikumar PG, Ramachandra M. Small molecule agents targeting PD-1 checkpoint pathway for cancer immunotherapy: mechanisms of action and other considerations for their advanced development. Front Immunol. 2022;13:752065.
5 Wang Y, Zhang N, Wang F, Li Z. Abstract LB-018: orally active small molecule PD-L1 inhibitor demonstrating similar efficacy as Durvalumab in human knock-in MC38 mode. Proceedings: AACR annual meeting 2019; March 29–April 3. Atlanta (GA): 2019.
6 Le Biannic R, Magnez R, Klupsch F, Leleu-Chavain N, Thiroux B, Tardy M, et al. Pyrazolones as inhibitors of immune checkpoint blocking the PD-1/PD-L1 interaction. Eur J Med Chem. 2022;236:114343.
7 Lai F, Ji M, Huang L, Wang Y, Xue N, Du T, et al. YPD-30, a prodrug of YPD-29B, is an oral small-molecule inhibitor targeting PD-L1 for the treatment of human cancer. Acta Pharm Sin B. 2022;12(6):2845–58.
8 Konieczny M, Musielak B, Kocik J, Skalniak L, Sala D, Czub M, et al. Di-bromo-Based small-molecule inhibitors of the PD-1/PD-L1 immune checkpoint. J Med Chem. 2020;63(19):11271–85.
9 Shaabani S, Gadina L, Surmiak E, Wang Z, Zhang B, Butera R, et al. Biphenyl ether analogs containing pomalidomide as small-molecule inhibitors of the programmed cell death-1/programmed cell death-ligand 1 interaction. Molecules. 2022;27(11):3454.
10 Chen W, Huang Y, Pan W, Xu M, Chen L. Strategies for developing PD-1 inhibitors and future directions. Biochem Pharmacol. 2022;202:115113.
11 Zak KM, Kitel R, Przetocka S, Golik P, Guzik K, Musielak B, et al. Structure of the complex of human programmed death 1, PD-1, and its ligand PD-L1. Structure. 2015;23(12):2341–8.
12 Lee JY, Lee HT, Shin W, Chae J, Choi J, Kim SH, et al. Structural basis of checkpoint blockade by monoclonal antibodies in cancer immunotherapy. Nat Commun. 2016;7:13354.
13 Acúrcio RC, Leonardo-Sousa C, García-Sosa AT, Salvador JA, Florindo HF, Guedes RC. Structural insights and binding analysis for determining the molecular bases for programmed cell death protein ligand-1 inhibition. Medchemcomm. 2019;10:1810–8.
14 Zak KM, Grudnik P, Magiera K, Dömling A, Dubin G, Holak TA. Structural biology of the immune checkpoint receptor PD-1 and its ligands PD-L1/PD-L2. Structure. 2017;25(8):1163–74.
15 Kumar GS, Moustafa M, Sahoo AK, Malý P, Bharadwaj S. Computational investigations on the natural small molecule as an inhibitor of programmed death ligand 1 for cancer immunotherapy. Life. 2022;12(5):659.
16 Ashizawa T, Iizuka A, Tanaka E, Kondou R, Miyata H, Maeda C, et al. Antitumor activity of the PD-1/PD-L1 binding inhibitor BMS-202 in the humanized MHC-double knockout NOG mouse. Biomed Res. 2019;40(6):243–50.
17 Surmiak E, Magiera-Mularz K, Musielak B, Muszak D, Kocik-Krol J, Kitel R, et al. PD-L1 inhibitors: different classes, activities, and mechanisms of action. Int J Mol Sci. 2021;22(21):11797.
18 Magnez R, Thiroux B, Taront S, Segaoula Z, Quesnel B, Thuru X. PD-1/PD-L1 binding studies using microscale thermophoresis. Sci Rep. 2017;7(1):17623.
19 Leleu-Chavain N, Regnault R, Ahouari H, Le Biannic R, Kouach M, Klupsch F, et al. Antioxidant properties and aldehyde reactivity of PD-L1 targeted aryl-pyrazolone anticancer agents. Molecules. 2022;27(10):3316.
20 Bailly C, Vergoten G. Protein homodimer sequestration with small molecules: focus on PD-L1. Biochem Pharmacol. 2020;174:113821.
21 Bailly C, Vergoten G. Flurbiprofen as a biphenyl scaffold for the design of small molecules binding to PD-L1 protein dimer. Biochem Pharmacol. 2020;178:114042.
22 Bailly C, Vergoten G. N-glycosylation and ubiquitinylation of PD-L1 do not restrict interaction with BMS-202: a molecular modeling study. Comput Biol Chem. 2020;88:107362.
23 Cha PH, Cho YH, Lee SK, Lee J, Jeong WJ, Moon BS, et al. Small-molecule binding of the axin RGS domain promotes β-catenin and Ras degradation. Nat Chem Biol. 2016;12(8):593–600.
24 Cha PH, Choi KY. Simultaneous destabilization of β-catenin and Ras via targeting of the axin-RGS domain as a potential therapeutic strategy for colorectal cancer. BMB Rep. 2016;49(9):455–6.

25 Zak KM, Grudnik P, Guzik K, Zieba BJ, Musielak B, Dömling A, et al. Structural basis for small molecule targeting of the programmed death ligand 1 (PD-L1). Oncotarget. 2016;7(21):30323–35.
26 Jorgensen WL, Tirado-Rives J. Molecular modeling of organic and biomolecular systems using BOSS and MCPRO. J Comput Chem. 2005;26(16):1689–700.
27 Vergoten G, Mazur I, Lagant P, Michalski JC, Zanetta JP. The SPASIBA force field as an essential tool for studying the structure and dynamics of saccharides. Biochimie. 2003;85(1–2):65–73.
28 Lagant P, Nolde D, Stote R, Vergoten G, Karplus M. Increasing normal modes analysis accuracy: the SPASIBA spectroscopic force field introduced into the CHARMM program. J Phys Chem A. 2004;108(18):4019–29.
29 Shimozono S, Miyawaki A. Engineering FRET constructs using CFP and YFP. Methods Cel Biol. 2008;85:381–93.
30 Marasco M, Berteotti A, Weyershaeuser J, Thorausch N, Sikorska J, Krausze J, et al. Molecular mechanism of SHP2 activation by PD-1 stimulation. Sci Adv. 2020;6(5):4458.
31 Chen R, Yuan D, Ma J. Advances of biphenyl small-molecule inhibitors targeting PD-1/PD-L1 interaction in cancer immunotherapy. Future Med Chem. 2022;14(2):97–113.
32 Muszak D, Surmiak E, Plewka J, Magiera-Mularz K, Kocik-Krol J, Musielak B, et al. Terphenyl-based small-molecule inhibitors of programmed cell death-1/programmed death-ligand 1 protein-protein interaction. J Med Chem. 2021;64(15):11614–36.
33 Wang T, Cai S, Wang M, Zhang W, Zhang K, Chen D, et al. Novel biphenyl pyridines as potent small-molecule inhibitors targeting the programmed cell death-1/programmed cell death-ligand 1 interaction. J Med Chem. 2021;64(11):7390–403.
34 Butera R, Ważyńska M, Magiera-Mularz K, Plewka J, Musielak B, Surmiak E, et al. Design, synthesis, and biological evaluation of imidazopyridines as PD-1/PD-L1 antagonists. ACS Med Chem Lett. 2021;12(5):768–73.
35 Kamalinia G, Engel BJ, Srinivasamani A, Grindel BJ, Ong JN, Curran MA, et al. mRNA display Discovery of a novel programmed death ligand 1 (PD-L1) binding peptide (a peptide ligand for PD-L1). ACS Chem Biol. 2020;15(6):1630–41.
36 Xaypraseuth A, Madahar V, Liao J. Development of quantitative förster resonance energy transfer (qFRET) based high throughput (HTS) screening for PD-1/PD-L1 immune-checkpoint assay. UC Riverside Undergraduate Res J Submit. 2020;14(1):87–93.
37 Synthesis of KYA1797K via Knoevenagel condensation. https: //www.reddit.com/r/chemistry/comments/65l5ax/synthesis_of_kya1797k_via_knoevenagel/.
38 Jeong WJ, Ro EJ, Choi KY. Interaction between Wnt/β-catenin and RAS-ERK pathways and an anti-cancer strategy via degradations of β-catenin and RAS by targeting the Wnt/β-catenin pathway. NPJ Precis Oncol. 2018;2(1):5.
39 Lee SK, Cho YH, Cha PH, Yoon JS, Ro EJ, Jeong WJ, et al. A small molecule approach to degrade RAS with EGFR repression is a potential therapy for KRAS mutation-driven colorectal cancer resistance to cetuximab. Exp Mol Med. 2018;50(11):1–12.
40 Park J, Cho YH, Shin WJ, Lee SK, Lee J, Kim T, et al. A Ras destabilizer KYA1797K overcomes the resistance of EGFR tyrosine kinase inhibitor in KRAS-mutated non-small cell lung cancer. Sci Rep. 2019;9(1):648.
41 Hahn S, Lee MR, Han J, Kim MK, Oh SH, Lyu CJL. Inhibition of acute leukemia by a small molecule KYA1797K which destabilize RAS and β-catenin. Blood. 2019;134(Suppl_1):5758.
42 Wagstaff M, Coke B, Hodgkiss GR, Morgan RG. Targeting β-catenin in acute myeloid leukaemia: past, present, and future perspectives. Biosci Rep. 2022;42(4):BSR20211841.
43 Ryu WJ, Lee JE, Cho YH, Lee G, Seo MK, Lee SK, et al. A therapeutic strategy for chemotherapy-resistant gastric cancer via destabilization of both β-catenin and RAS. Cancers (Basel). 2019;11(4):496.
44 Ryu WJ, Lee JD, Park JC, Cha PH, Cho YH, Kim JY, et al. Destabilization of β-catenin and RAS by targeting the Wnt/β-catenin pathway as a potential treatment for triple-negative breast cancer. Exp Mol Med. 2020;52(5):832–42.
45 Ryu WJ, Han G, Lee SH, Choi KY. Suppression of Wnt/β-catenin and RAS/ERK pathways provides a therapeutic strategy for gemcitabine-resistant pancreatic cancer. Biochem Biophys Res Commun. 2021;549:40–6.
46 Choi SY, Pi JH, Park SK, Kang CJ. Crlz-1 controls germinal center reaction by relaying a Wnt signal to the bcl-6 expression in centroblasts during humoral immune responses. J Immunol. 2019;203(10):2630–43.
47 Wang YQ, Wang NX, Luo Y, Yu CY, Xiao JH. Ganoderal A effectively induces osteogenic differentiation of human amniotic mesenchymal stem cells via cross-talk between Wnt/β-catenin and BMP/SMAD signaling pathways. Biomed Pharmacother. 2020;123:109807.
48 Yan G, Li S, Yue M, Li C, Kang Z. Lysine demethylase 5B suppresses CC chemokine ligand 14 to promote progression of colorectal cancer through the Wnt/β-catenin pathway. Life Sci. 2021;264:118726.
49 Zhang S, Jin S, Zhang S, Li YY, Wang H, Chen Y, et al. Vitexin protects against high glucose-induced endothelial cell apoptosis and oxidative stress via Wnt/β-catenin and Nrf2 signalling pathway. Arch Physiol Biochem. 2022:1–10.
50 Cha PH, Hwang JH, Kwak DK, Koh E, Kim KS, Choi KY. APC loss induces Warburg effect via increased PKM2 transcription in colorectal cancer. Br J Cancer. 2021;124(3):634–44.
51 Chang J, Xavier HW, Chen D, Liu Y, Li H, Bian Z. Potential role of traditional Chinese medicines by wnt/β-catenin pathway compared with targeted small molecules in colorectal cancer therapy. Front Pharmacol. 2021;12:690501.
52 Ruan Z, Liang M, Lai M, Shang L, Deng X, Su X. KYA1797K down-regulates PD-L1 in colon cancer stem cells to block immune evasion by suppressing the β-catenin/STT3 signaling pathway. Int Immunopharmacol. 2020;78:106003.
53 Jiang H, Fan M, Wang J, Sarma A, Mohanty S, Dokholyan NV, et al. Guiding conventional protein-ligand docking software with convolutional neural networks. J Chem Inf Model. 2020;60(10):4594–602.
54 Pu J, He X, Xu W, Wang C, Lan Q, Hua C, et al. The analogs of furanyl methylidene rhodanine exhibit broad-spectrum inhibitory and inactivating activities against enveloped viruses, including SARS-CoV-2 and its variants. Viruses. 2022;14(3):489.